



# Nonlocal maximum likelihood estimation method for denoising multiple-coil magnetic resonance images

Jeny Rajan<sup>a,\*</sup>, Jelle Veraart<sup>a</sup>, Johan Van Audekerke<sup>b</sup>, Marleen Verhoye<sup>b</sup>, Jan Sijbers<sup>a</sup>

<sup>a</sup>IBBT-Vision Lab, Department of Physics, University of Antwerp, Belgium, 2610

<sup>b</sup>Bio-Imaging Lab, Department of Biomedical Sciences, University of Antwerp, Belgium, 2610

Received 13 December 2011; revised 26 March 2012; accepted 18 April 2012

## Abstract

Effective denoising is vital for proper analysis and accurate quantitative measurements from magnetic resonance (MR) images. Even though many methods were proposed to denoise MR images, only few deal with the estimation of true signal from MR images acquired with phased-array coils. If the magnitude data from phased array coils are reconstructed as the root sum of squares, in the absence of noise correlations and subsampling, the data is assumed to follow a non central- $\chi$  distribution. However, when the  $k$ -space is subsampled to increase the acquisition speed (as in GRAPPA like methods), noise becomes spatially varying. In this note, we propose a method to denoise multiple-coil acquired MR images. Both the non central- $\chi$  distribution and the spatially varying nature of the noise is taken into account in the proposed method. Experiments were conducted on both simulated and real data sets to validate and to demonstrate the effectiveness of the proposed method.

© 2012 Elsevier Inc. All rights reserved.

**Keywords:** MRI; Noise; Denoising; NLML; Non central chi distribution

## 1. Introduction

Stochastic noise is one of the main causes of quality deterioration in magnetic resonance (MR) images, and hence, estimation and removal of noise remains an active area of research. Consideration of how noise affects the true signal is important for proper interpretation and analysis of MR images [1]. Noise in the MRI can be naturally reduced by averaging complex images after multiple acquisitions. This, however, may not be feasible in clinical and small animal MR imaging (MRI) where there is an increasing need for speed. Also, time-sensitive acquisitions in contrast material-enhanced studies, functional studies, diffusion MRI or studies with limited imaging time, experiments cannot be repeated to do averaging. Thus, post processing techniques to remove noise in the magnitude image is important. It is usually assumed that the noise in the MRI  $k$ -space data from each receiver channel is normally distributed. Due to the orthogonality of the Fourier basis functions,

the noise remains Gaussian distributed after an inverse Fourier transform. However, the subsequent nonlinear operation, being the computation of the root of the sum of squares (SoS) of the Gaussian distributed complex image(s), leads to a magnitude image, which is no longer Gaussian distributed. In single coil systems, such magnitude data is governed by a stationary Rician distribution. For multi-coil systems, the magnitude image is non central Chi (nc- $\chi$ ) distributed, provided that the  $k$  space was fully sampled and no correlations between the coil data exists [2,3]. Multiple coil systems were initially developed to enhance the signal-to-noise ratio (SNR) of the acquired images and later parallel MRI (pMRI) techniques were employed to it to accelerate the acquisition process through  $k$ -space subsampling. Nevertheless, the subsampling of  $k$ -space can cause the noise in the magnitude image to be non-stationary.

In the recent past, several adaptive filtering techniques to improve the quality of magnitude MR images have been proposed [4–9]. The Rician nature of the noise was incorporated in most of these methods to make it a suitable candidate for denoising magnitude MR images. However, none of the aforementioned methods are adapted to deal with nc- $\chi$  distributed data. Employing a Rician model to describe

\* Corresponding author.

E-mail address: [jeny.rajan@ua.ac.be](mailto:jeny.rajan@ua.ac.be) (J. Rajan).

nc- $\chi$  distributed data (if the number of coils  $>1$ ) may, however, introduce a bias in the estimated parameters. This bias will increase with increasing number of coils. However, multi-channel MRI acquisition schemes with pMRI techniques are becoming increasingly popular. Very recently, Brion et al [10] proposed a method to estimate the underlying true signal from nc- $\chi$  distributed data. In their paper, a linear minimum mean square estimator (LMMSE) method was used to estimate the true underlying intensity. In this technical note, a recently proposed nonlocal maximum likelihood (NLML) estimation method [11] is extended to deal with nc- $\chi$  distributed and the spatially varying nature of the noise, which significantly increases its applicability.

In Sections 2 and 3, the theory behind the denoising method is clarified. In Section 4, results are shown on simulated as well as experimental MR images. Finally, conclusions are drawn in Section 5.

## 2. Theory

In a multiple-coil MR acquisition system, the acquired signal in the presence of noise in each coil can be typically modeled as a complex Gaussian process. Thus, the complex signal in each coil  $l$  (for  $l=1,2,\dots,L$ ) after the inverse Fourier transform can be expressed as [3].

$$C_l(\mathbf{x}) = S_l(\mathbf{x}) + n_l(\mathbf{x}; \sigma_g^2) \quad (1)$$

where  $S_l(\mathbf{x})$  represents the true complex signal in the absence of noise for each coil  $l$  and  $n_l(\mathbf{x}; \sigma_g^2) = n_{l_r}(\mathbf{x}; \sigma_g^2) + jn_{l_i}(\mathbf{x}; \sigma_g^2)$ , the complex Gaussian noise in each coil  $l$ . If no subsampling is done, the composite magnitude signal  $M(\mathbf{x})$  can be written as [3,12].

$$M(\mathbf{x}) = \sqrt{\sum_{l=1}^L |C_l(\mathbf{x})|^2} \quad (2)$$

Assuming absence of noise correlation and that the  $L$  coils are statistically independent, the probability density function (PDF) of the composite magnitude signal,  $M$ , follows a nc- $\chi$  distribution defined by [12]:

$$p(M) = \frac{A}{\sigma_g^2} \left( \frac{M}{A} \right)^L e^{-\frac{A^2 + M^2}{2\sigma_g^2}} I_{L-1} \left( \frac{AM}{\sigma_g^2} \right) \quad (3)$$

where  $A$  is the underlying true composite magnitude signal in the absence of noise,  $\sigma_g^2$ , the variance of the Gaussian noise in the complex data which is assumed to be the same for all  $L$  channels and  $I_{L-1}$  is the  $(L-1)^{th}$  order modified Bessel function of the first kind.

## 3. Methods

The objective of the proposed method is to estimate the true underlying intensity  $A$  from the composite magnitude

image in which the observations follow a nc- $\chi$  distribution. For this purpose, we extended the NLML method which was originally proposed for denoising images with Rician noise.

### 3.1. Extended NLML method

Let  $M_1, M_2, \dots, M_n$  be  $n$  i.i.d nc- $\chi$  observations. Then the joint PDF of the observation is

$$p(\{M_i\} | A) = \prod_{i=1}^n \frac{A}{\sigma_g^2} \left( \frac{M_i}{A} \right)^L e^{-\frac{A^2 + M_i^2}{2\sigma_g^2}} I_{L-1} \left( \frac{AM_i}{\sigma_g^2} \right) \quad (4)$$

Given the observed data and a model of interest, the unknown parameters in the PDF can be estimated by maximizing the corresponding likelihood function. The unknown parameter in Eq. (4) is the true underlying intensity  $A$ . However, if  $\sigma_g^2$  is not known in advance, it can also be estimated along with  $A$  by maximizing the likelihood function  $\mathcal{L}$  or equivalently  $\ln \mathcal{L}$ , with respect to  $A$  and  $\sigma_g^2$ :

$$\{\hat{A}_{ML}, \hat{\sigma}_{ML}^2\} = \arg \left\{ \max_{A, \sigma_g^2} (\ln \mathcal{L}) \right\} \quad (5)$$

where

$$\begin{aligned} \ln \mathcal{L} = & n \ln \left( \frac{A}{\sigma_g^2} \right) + L \sum_{i=1}^n \ln \left( \frac{M_i}{A} \right) - \sum_{i=1}^n \left( \frac{M_i^2 + A^2}{2\sigma_g^2} \right) \\ & + \sum_{i=1}^n \ln I_{L-1} \left( \frac{AM_i}{\sigma_g^2} \right) \end{aligned} \quad (6)$$

and  $\hat{A}_{ML}$  and  $\hat{\sigma}_{ML}^2$  are the estimated underlying true intensity and the noise variance respectively. Nevertheless, to estimate  $\hat{A}_{ML}$  and  $\hat{\sigma}_{ML}^2$  for each pixel in the image using Eq. (5), samples  $\{M_i\}$  with identical underlying intensity and noise variance need to be selected. The straightforward approach to select samples  $\{M_i\}$  is to select all pixels from a local neighborhood. However, it is clear that around edges and fine structures the assumption of uniform underlying intensity is violated, and, as a result, blurring will be introduced in the image. An alternate approach is to use non local (NL) pixels instead [11]. The NL pixels are selected based on the intensity similarity of the pixel neighborhood. If the neighborhoods of two pixels are similar, then their central pixels should have a similar meaning and thus similar gray values [13]. The similarity of the pixel neighborhoods can be computed by taking the intensity distance (Euclidian distance) between them [11]:

$$d_{i,j} = ||N_i - N_j|| \quad (7)$$

where  $d_{i,j}$  is the intensity distance between the neighborhoods  $N_i$  and  $N_j$  of the pixels  $i$  and  $j$ . For each pixel  $i$ , the intensity distance  $d$  between  $i$  and all other non local pixels  $j$  as defined by Eq. (7), in the search window are measured. The first  $k$  pixels are then selected as  $\{M_i\}$  after sorting the NL pixels in the increasing order of the distance  $d$  for the maximum likelihood (ML) estimation. Even though, in

theory the search window is the whole image, for complexity reasons most implementations restrict the search area to a window surrounding  $i$ . In our implementation, a search window of size  $11 \times 11 \times 11$  was used.

If the noise level is spatially invariant, the noise standard deviation,  $\sigma_g$ , can be estimated from the background region of the image. This  $\sigma_g$  can be used in Eq. (6) to estimate the underlying true intensity A. Estimating A using ML with a known  $\sigma_g$  converges faster and will be more precise than estimating both A and  $\sigma_g$  simultaneously. The noise level can be estimated from the background as:

$$\hat{\sigma}_g = \sqrt{\frac{2}{\pi} \frac{2^{L-1}(L-1)!}{(2L-1)!!}} \langle M_B \rangle \quad (8)$$

where  $\langle M_B \rangle$  is the mean of the central  $\chi$  distributed background region. An explicit segmentation is needed in this case to extract the background regions, which can be sometimes difficult. Also, artifacts (e.g. Ghost artifacts) can influence the estimation. Explicit segmentation, and to some extent, the influence of artifacts can be avoided by using the local statistics for noise estimation as suggested in [3] as:

$$\hat{\sigma}_g = \sqrt{\frac{2}{\pi} \frac{2^{L-1}(L-1)!}{(2L-1)!!}} \text{mode}\{\langle M_B(i) \rangle\} \quad (9)$$

where  $\langle M_B(i) \rangle$  corresponds to the local mean computed for each pixel  $i$  in the image.

### 3.2. Estimation of the number of coils L

An important parameter in the nc- $\chi$  PDF is the number of coils L. Usually the experimenter knows L in advance. However, L can also be computed from the data statistics. If the k-space is not subsampled and if the background pixels in the acquired magnitude image follow a central  $\chi$  distribution, then the number of coils can be estimated from the SNR of the background region (the ratio of the mean of the central  $\chi$  distributed background region and its standard deviation). This SNR from the background region will be constant for a particular L [2,14]. This can be easily proved from the moments of the central- $\chi$  distribution.

Let  $M_B$  represent the background region of the composite magnitude image. Then the first and second moments of  $M_B$  can be written as [12,14]:

$$\langle M_B \rangle = \beta_L \sigma_g \quad (10)$$

and

$$\langle M_B^2 \rangle = 2L\sigma_g^2 \quad (11)$$

where

$$\beta_L = \sqrt{\frac{\pi}{2} \frac{(2L-1)!!}{2^{L-1}(L-1)!}} \quad (12)$$

The variance of  $M_B$  in terms of the moments can be written as:

$$\sigma_{M_B}^2 = \langle M_B^2 \rangle - \langle M_B \rangle^2 \quad (13)$$

Substituting Eq. (10) and Eq. (11) in Eq. (13) yields.

$$\sigma_g = \frac{\sigma_{M_B}}{\sqrt{2L-\beta_L^2}} \quad (14)$$

Now by substituting Eq. (14) in Eq. (10) we can compute the SNR as:

$$\frac{\langle M_B \rangle}{\sigma_{M_B}} = \frac{\beta_L}{\sqrt{2L-\beta_L^2}} \quad (15)$$

This SNR will always be a constant for a particular value of L as long as the background follows a central- $\chi$  distribution. SNR for different values of L computed using Eq. (15) is given in Table 1. In summary, L can be predicted by measuring the SNR of the background region of the image. However, when the k-space is subsampled or if there exists correlation between the data from different coils, then the background region will not strictly follow a central- $\chi$  distribution and as a result the values in Table 1 may not hold. This is discussed in detail in the work of Aja-Fernández et al. [15].

## 4. Experiments and Results

Synthetic experiments for image denoising were carried out on the standard BrainWeb MR volume [16]. In the first experiment, a synthetic image was created by multiplying the BrainWeb image with eight complex-valued coil sensitivities. Gaussian noise was then added to the real and imaginary parts of the image from each coil before creating the final magnitude image using the SoS method. Due to the SoS operation, the noise in the magnitude image follows a nc- $\chi$  distribution. This noisy image is then denoised with the proposed method and also with the LMMSE method in [10], which was recently proposed for denoising nc- $\chi$  distributed MR images. The denoising methods were executed with the following parameters.(i) proposed method : search window size :  $11 \times 11 \times 11$ , neighborhood size :  $3 \times 3 \times 3$  and sample size  $k = 20$  (ii) LMMSE : window size:  $5 \times 5 \times 5$ . The noise variance  $\sigma_g^2$  used in both methods was estimated using Eq. (9).

The visual quality comparison of the methods can be made from the results given in Fig. 1. In visual analysis, the expectations are (i) perceptually flat regions should be as

Table 1  
SNR of the central- $\chi$  distributed background region for different values of L

L	1	2	4	8	16	32	64
SNR	1.9131	2.7548	3.9429	5.6146	7.9694	11.2918	15.9845

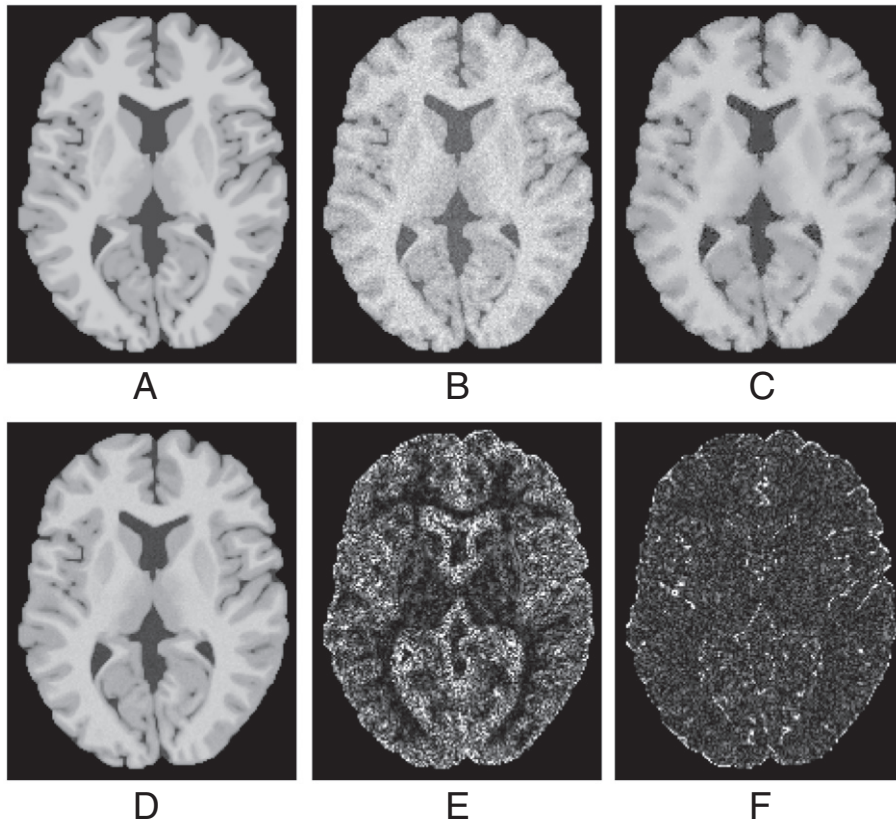


Fig. 1. Denoising of MRI with nc- $\chi$  distributed noise. (A) Ground Truth reconstructed with SoS method with  $L=8$  (B) Ground Truth corrupted with nc- $\chi$  distributed noise of  $\sigma_g = 15$  (C) denoised with LMMSE method (D) denoised with proposed method (E) and (F) corresponding residual images of (C) and (D) (scale 0-25).

smooth as possible (ii) image edges and corners should be well preserved (iii) texture detail should not be lost and (iv) few or ideally no artifacts [11,17]. It can be observed from Fig. 1 that the image denoised with the proposed method is closer to the original one (based on the above mentioned criteria) than the image denoised with the LMMSE approach. This is clearly visible from the residual images. For quantitative analysis, the experiment was repeated with various values of  $\sigma_g$  varying from 5 to 30

and the results based on PSNR and mean SSIM [18] are given in the Table 2. In the quantitative analysis, the background region was excluded; that is, only the area of the image inside the skull was considered. The values in Table 2 highlight the effectiveness of the proposed method for denoising nc- $\chi$  data.

In the second experiment, synthetic images were reconstructed with SoS, SENSE [19] and GRAPPA [20] method using 4 coils. For SENSE and GRAPPA an acceleration factor of 2 were used. Gaussian noise of standard deviation,  $\sigma_g = 10$ , was added to the complex synthetic image (4 complex images with different sensitivities) to create the noisy image. The SoS image was reconstructed from the complex images by taking the root sum of squares. For SENSE and GRAPPA reconstruction experiment, the complex k-space images were created by taking the Fourier transform of the complex noisy image. These k-space images were then subsampled with a factor of 2. SENSE and GRAPPA methods were then applied to reconstruct the images from the subsampled k-space images. The PULSAR toolbox [21] was used for the SENSE and GRAPPA reconstruction. The proposed denoising algorithm was then applied over all the 3 reconstructed magnitude images (i.e., SoS, SENSE and GRAPPA). In the case of denoising SENSE reconstructed images, the number of coils

Table 2  
Quantitative analysis of the proposed method with LMMSE method proposed in [10]

$\sigma_g$	5	10	15	20	25	30
Noisy						
PSNR	35.23	28.15	23.29	19.73	16.87	14.48
MSSIM	0.9318	0.8129	0.6938	0.5978	0.5157	0.4466
LMMSE						
PSNR	37.05	32.42	30.12	28.95	28.11	27.45
MSSIM	0.9618	0.9131	0.8703	0.8407	0.8155	0.7882
Proposed						
PSNR	36.01	35.38	34.01	32.27	30.45	28.71
MSSIM	0.9706	0.9612	0.9371	0.9021	0.8612	0.8118

This experiment was conducted on the synthetic image of the brain reconstructed with SoS method with  $L=8$ .

$L$  should be taken as 1, since the final magnitude image is generated from only 1 complex (composite) image. Hence in SENSE reconstructed images, the noise will be Rician distributed (which is a special case of  $nc\text{-}\chi$  with  $L=1$ ), but spatially varying. The result of this experiment is shown in Fig. 2.

It can be observed from the results that the proposed method performs well in all the cases. However, there is some bias in the denoised image of the GRAPPA reconstructed image which is visible in the residual image. This bias is because of the influence of the signal correlation

in  $L$ . The denoising experiment was executed with a constant value for  $L$  (in this case  $L=4$ ). Even if the coils are initially uncorrelated (which was the case in our simulations), signals will be correlated due to GRAPPA reconstruction [22]. The correlation will increase with the increase in the number of coils used for image acquisition. Correlations will affect the number of degrees of freedom of the distribution [15]. As a result, the value of the number of coils,  $L$ , will reduce and vary across the image. Ignoring effective  $L$  can thus create bias in the denoised image especially when there is high signal correlation. However, estimation of effective  $L$

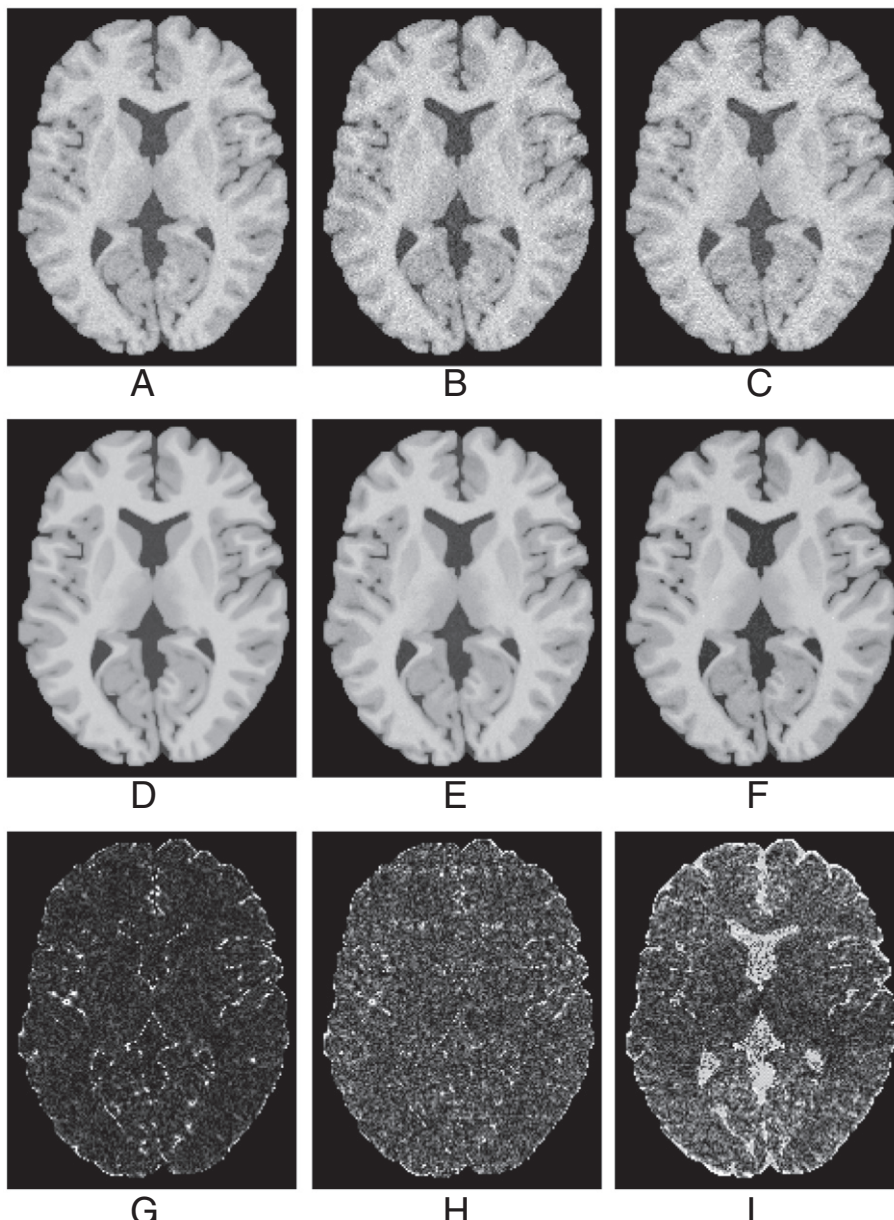


Fig. 2. Denoising of multiple-coil acquired MRI. (A) [PSNR: 29.49,MSSIM: 0.8256], (B) [PSNR: 24.44,MSSIM: 0.6749] and (C) [PSNR: 24.77,MSSIM: 0.6848] are images acquired with  $L=4$  and  $\sigma_g=10$  and reconstructed with SoS, SENSE (acceleration factor: 2) and GRAPPA (acceleration factor: 2) respectively. (D) [PSNR: 34.88, MSSIM: 0.9714], (E) [PSNR: 31.81, MSSIM: 0.9079] and (F) [PSNR: 28.41, MSSIM : 0.9111] are the denoised images of SoS, SENSE and GRAPPA reconstructed images. (G), (H) and (I) are the corresponding residual images (scale 0-25) with respect to the Ground Truth.

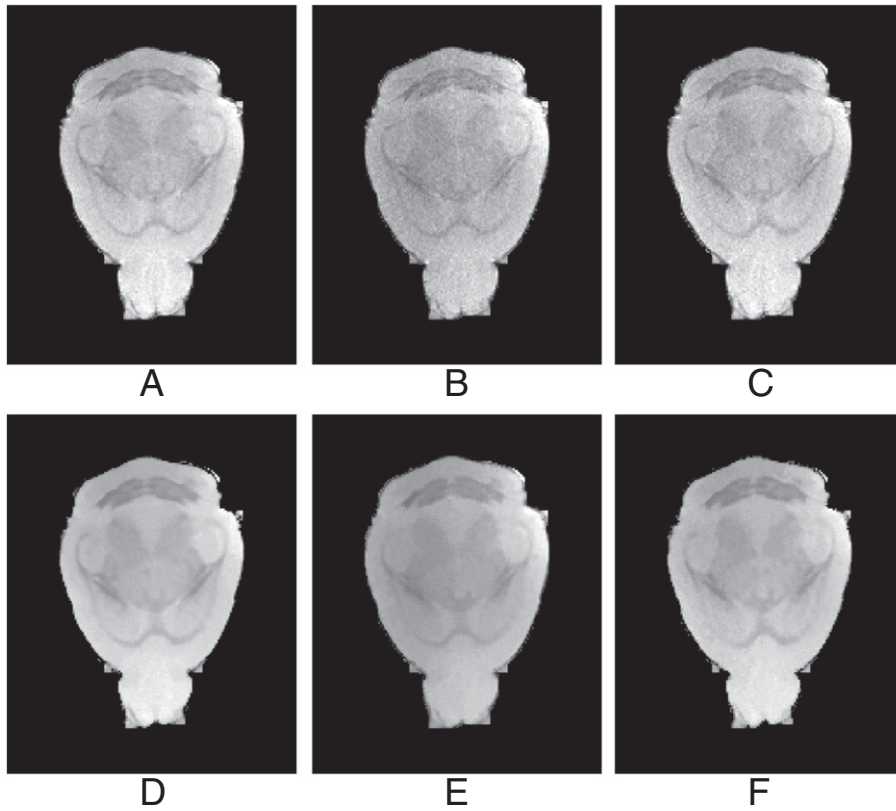


Fig. 3. Experiments on ex vivo mice images. (A) (B) and (C) original mice image acquired with  $2 \times 2$  channel phased array coil and reconstructed with SoS, SENSE and GRAPPA. (D), (E) and (F) are the corresponding denoised images using the proposed method.

requires raw MR data from each coil. Also, maximum likelihood estimation might not converge properly when the selected samples doesn't exactly follows the nc- $\chi$  distribution (especially when estimating  $A$  and  $\sigma$  simultaneously with a large  $L$ ).

For the experiments on the real data, we acquired ex vivo MR images (2D) of a mouse brain with a  $2 \times 2$  channel phased array coil using Bruker 7.0T scanner. The images were acquired with SoS and GRAPPA (with an acceleration factor of 2) and later an image was also reconstructed with SENSE (with an acceleration factor of 2) from the raw data using the PULSAR tool box. The proposed denoising method was then applied on all the three reconstructed images. The results are shown in Fig. 3. This experiment on the real data set additionally indicates the effectiveness of the proposed method. We also analyzed the background region of the acquired SoS image to check whether there is any significant correlation between the data from different coils. If there is no significant correlation, the background region of the SoS image should follow a central- $\chi$  distribution. Fig. 4 shows the distribution of the background region of the mouse brain image acquired with SoS method. Comparison with the true central- $\chi$  distribution shows that there is no significant correlation between the signals from different coils in this case.

## 5. Conclusion

We have proposed a method to denoise MR images in which the data follows a nc- $\chi$  distribution. The proposed method is an extension of the NLML method which was proposed for denoising images corrupted with Rician noise. We extended this method to nc- $\chi$  distributed data and also the spatially varying nature of the noise is incorporated.

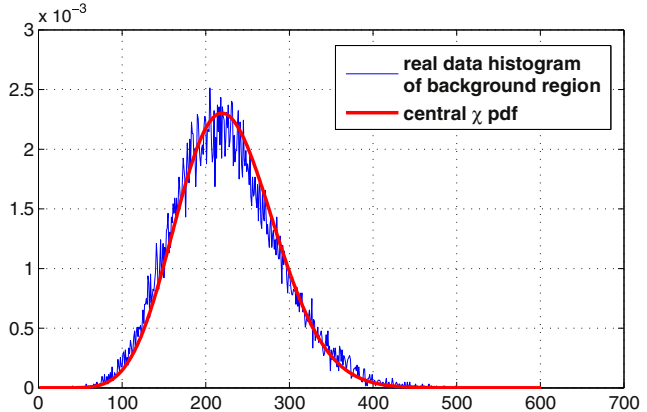


Fig. 4. Actual distribution of the background region of the mice image (acquired with SoS with  $L=4$ ) compared with the central- $\chi$  PDF (with  $L=4$  and  $\sigma_g$  estimated from the background region of the image).

Experiments were conducted on both simulated and real images. The experimental results shows that the proposed method is very effective for MR images which follows nc- $\chi$  distribution.

## Acknowledgments

This work was financially supported by the Inter-University Attraction Poles Program 6-38 of the Belgian Science Policy, and by the SBO-project QUANTIVIAM (060819) of the Institute for the Promotion of Innovation through Science and Technology in Flanders (IWT-Vlaanderen).

## References

- [1] Landman BA, Bazin PL, Prince JL. Estimation and application of spatially variable noise fields in diffusion tensor imaging. *Magn Reson Imaging* 2009;27:741–51.
- [2] Dietrich O, Raya JG, Reeder SB, Ingrisch M, Reiser MF, Schoenberg SO. Influence of multichannel combination, parallel imaging and other reconstruction techniques on MRI noise characteristics. *Magn Reson Imaging* 2008;26:754–62.
- [3] Aja-Fernández S, Tristán A, Alberola-López C. Noise estimation in single and multiple coil magnetic resonance data based on statistical models. *Magn Reson Imaging* 2009;27:1397–409.
- [4] Sijbers J, den Dekker AJ, Van der Linden A, Verhoye M, Van Dyck D. Adaptive anisotropic noise filtering for magnitude MR data. *Magn Reson Imaging* 1999;17:1533–9.
- [5] Manjón JV, Carbonell-Caballero J, Lull JJ, García-Martí G, Martí-Bonmatí L, Robles M. MRI denoising using non local means. *Med Image Anal* 2008;12:514–23.
- [6] Krissian K, Aja-Fernández S. Noise driven anisotropic diffusion filtering of MRI. *IEEE Trans Image Proc* 2009;18:2265–74.
- [7] Manjón JV, Coupé P, Martí-Bonmatí L, Collins DL, Robles M. Adaptive non local means denoising of MR images with spatially varying noise levels. *J Magn Reson Imaging* 2010;31:192–203.
- [8] Rajan J, Jeurissen B, Verhoye M, Van Audekerke J, Sijbers J. Maximum likelihood estimation-based denoising of magnetic resonance images using restricted local neighborhoods. *Phys Med Biol* 2011;56:5221–34.
- [9] Rajan J, Van Audekerke J, Van der Linden A, Verhoye M, Sijbers J. An adaptive non local maximum likelihood estimation method for denoising magnetic resonance images. International Symposium on Biomedical Imaging; 2012. p. 1136–9.
- [10] Brion V, Poupon C, Riff O, Aja-Fernández S, Tristán-Vega A, Mangin JF, et al. Parallel MRI noise correction: an extension of LMMSE to non central  $\chi$  distributions. Medical Image Computing and Computer-Assisted Intervention - MICCAI 2011. Berlin: Springer-Verlag; 2011. p. 226–33.
- [11] He L, Greenshields IR. A nonlocal maximum likelihood estimation method for Rician noise reduction in MR images. *IEEE Trans Med Imaging* 2009;28:165–72.
- [12] Constantinides CD, Atalar E, McVeigh ER. Signal-to-noise measurements in magnitude images from NMR phased arrays. *Magn Reson Med* 1997;38:852–7.
- [13] Zimmer S, Didas S, Weickert J. A rotationally invariant block matching strategy improving image denoising with non-local means. International Workshop on Local and Non-Local Approximation in Image Processing, Switzerland; 2008. p. 135–42.
- [14] Koay CG, Basser PJ. Analytically exact correction scheme for signal extraction from noisy magnitude MR signals. *J Magn Reson* 2006;179:317–22.
- [15] Aja-Fernández S, Tristán-Vega A. Influence of noise correlation in multiple-coil statistical models with sum of squares reconstruction. *Magn Reson Med* 2011;67(2):580–5, <http://dx.doi.org/10.1002/mrm.23020> [Epub 2011 Jun 7].
- [16] Cocosco CA, Kollokian V, Kwan RS, Evans AC. 1997. Brainweb: Online interface to a 3D MRI simulated brain database; <http://www.bic.mni.mcgill.ca/brainweb/>. *NeuroImage* 5, S425.
- [17] Chen Q, Sun Q, Xia D. Homogeneity similarity based image denoising. *Pattern Recogn* 2010;43:4089–100.
- [18] Wang Z, Bovik A, Sheikh HR, Simoncelli EP. Image quality assessment: from error visibility to structural similarity. *IEEE Trans Image Proc* 2004;13:600–12.
- [19] Pruessmann KP, Weiger M, Scheidegger MB, Boesiger P. SENSE : Sensitivity encoding for fast MRI. *Magn Reson Med* 1999;42:952–62.
- [20] Griswold MA, Jacob PM, Heidemann R, Nittka M, Wang V, Kiefer B, et al. Generalized autocalibrating partially parallel acquisitions-GRAPPA. *Magn Reson Med* 2002;47:1202–10.
- [21] Ji JX, Son JB, Rane SD. PULSAR: a Matlab toolbox for parallel magnetic resonance imaging using array coils and multiple channel receivers. *Concepts Magn Reson Part B : Magn Reson Eng* 2007;31B(1):24–36.
- [22] Aja-Fernández S, Tristán-Vega A, Hoge WS. Statistical noise analysis in GRAPPA using a parametrized noncentral chi approximation model. *Magn Reson Med* 2011;65:1195–206.